Population transfer via adiabatic passage in the rubidium quantum ladder system

D. J. Maas, C. W. Rella, P. Antoine, E. S. Toma, and L. D. Noordam*
FOM–Instituut voor Atoom- en Molecuulfysica, Kruislaan 407, 1098 SJ Amsterdam, The Netherlands
(Received 13 July 1998)

Generally, high optical intensity is required for effective multiphoton excitation of quantum systems to highly excited states. In certain situations, however, lower-intensity, chirped pulses can provide more efficient transfer of population to the upper states by the process of adiabatic passage. We have studied the relative importance of these two mechanisms in the anharmonic $5s$-$5p$-$5d$ quantum ladder system of rubidium using frequency chirped laser pulses from an amplified Ti:sapphire laser ($\lambda=780$ and $\Delta\lambda=10$ nm). We measure simultaneously the three-photon ionization signal due to the Ti:sapphire and the population that remains in the $5d$ state with a postionizing 532-nm Nd:YAG pulse (where YAG denotes yttrium aluminum garnet). At low infrared fluences (80 μJ/cm^2), the transfer to the $5d$ state is significantly enhanced when the pulse frequency is swept from the red to the blue, such that it follows the frequency spacing of the rubidium ladder. Counterintuitively, population is also transferred efficiently for the blue-to-red chirp at high fluences (>5 mJ/cm^2). We attribute both of these effects to adiabatic passage from the $5s$ state to the $5d$ state. Even at the highest fluences, more efficient transfer occurs for either direction of chirp than occurs at zero chirp, where the intensity is maximal. A comparison to theoretical predictions reveals striking agreement in both absolute magnitude and functional form. These results have important implications for the understanding of population transfer in complex ladder systems, such as molecular anharmonic vibrational ladders.
[S1050-2947(99)01502-4]

PACS number(s): 42.50.Hz, 32.80.Bx, 32.80.Qk, 42.65.Re

I. INTRODUCTION

The manipulation of quantum systems through application of carefully shaped optical pulses has been an area of intense research in recent years. The advent of ultrafast laser systems that provide wide bandwidth transform-limited pulses, combined with the simultaneous development of powerful methods for the shaping and subsequent characterization of such pulses [1], has lead to the experimental realization of many early steps toward control of complex quantum-mechanical systems [2]. One important goal of quantum manipulation is the attempt to bring an ensemble of molecules into a specific highly excited vibrational state. This would facilitate the selective breaking of chemical bonds and thus allow control of chemical reactions [3,4]. There are several obstacles to overcome before this goal can be reached. Direct single-photon excitation of a highly excited vibrational state is not practical due to the small overlap between initial and final states. Therefore, stepwise excitation up the vibrational ladder is required, introducing other complications. Vibrational potentials are never purely harmonic, resulting in different transition frequencies for successive steps of the ladder and hence demanding the use of several excitation frequencies. Furthermore, the time scale for vibrational energy redistribution within the molecule is in the picosecond range.

Ultrashort laser pulses potentially represent a solution to these problems since the bandwidth of the pulses may be large enough to contain all the frequency components of the ladder and picosecond time resolution is readily obtained. At first glance, however, it may seem that selectivity cannot be sustained with this approach and even if the purpose is multiphoton dissociation, it turns out that the intensities needed to dissociate an appreciable fraction of the molecules are far beyond those leading to ionization. One possible solution to the problem is to employ frequency chirped ultrashort laser pulses [5]. Population transfer to the upper states is most efficiently accomplished when the instantaneous frequency of the laser pulse follows the spacing of the anharmonic vibrational ladder. This process is an example of chirped adiabatic passage. Observed in magnetic resonance, adiabatic passage (or adiabatic following) [6] is the process by which the quantum state of a system is changed by a slowly evolving, predominantly off-resonance optical field, rather than by direct on-resonance excitation, as is the case for Rabi pumping. Adiabatic passage is an attractive approach for obtaining efficient population transfer [2,7] primarily because, unlike Rabi pumping, it is relatively insensitive to inhomogeneities in the ensemble of molecules or variations in the optical field. Recently, population transfer via chirped pulse excitation has been experimentally studied in vibrational excitation of gas phase NO, where it was shown that population transfer to the $\nu=3$ vibrational level was enhanced by a factor of 10 by chirping the pulse appropriately [8]. In another series of measurements, the role of adiabatic passage was investigated in the cesium Rydberg series using chirped ultrafast far-infrared pulses [9].

However, due to the complexity of molecular systems and high quantum number Rydberg atoms, combined with the experimental difficulties inherent to the excitation and characterization of infrared transitions, it is impractical to study adiabatic passage throughout a full range of experimental conditions. For this reason, it is instructive to study in detail a theoretically and experimentally simpler system, the $5s \rightarrow 5p \rightarrow 5d$ anharmonic quantum ladder in the rubidium

*Author to whom correspondence should be addressed. FAX: +31 20 668 4106. Electronic address: noordam@amolf.nl

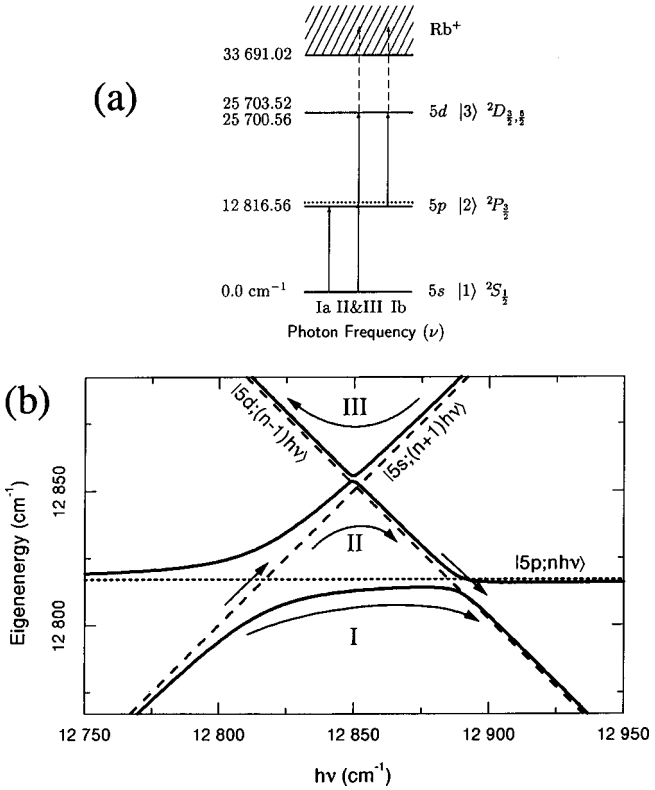

FIG. 1. (a) Simplified energy-level diagram of rubidium, showing the three levels of the anharmonic ladder and the continuum. The two transitions in the ladder can be driven by the same ultrashort optical pulse. (b) Dressed-atom diagram of the same levels, dressed as $|1+\hbar\omega\rangle$, $|2\rangle$, and $|3-\hbar\omega\rangle$. The dashed lines show the unperturbed energies as a function of the photon energy of the dressing field. The full lines show the dressed-atom energies when dipole coupling is included, for a laser intensity of 1.9×10^7 W/cm^2. The arrows indicate the different routes of excitation of the upper level ($5d$), as described in the text.

atom. In recent years, this system has been characterized in a number of experiments over a limited range of experimental conditions [10,11]. The results presented here, however, represent measurements made at both positive and negative chirps and throughout the full range of fluence, from the perturbative regime to saturation. Thus the role of adiabatic passage in population transfer in the rubidium anharmonic ladder system has been studied in a systematic way.

A simplified energy-level diagram of Rb is depicted in Fig. 1(a). Only the levels that play an important role in the experiment are shown. We label the $5s$, $5p$, and $5d$ states $|1\rangle$, $|2\rangle$, and $|3\rangle$, respectively. Note that these three states indeed form an anharmonic ladder, though both transitions can be accessed easily with a single Ti:sapphire laser pulse (see Fig. 3). In the experiment described here, the dependence of the population transfer to the upper level $|3\rangle$ on both the chirp of the laser pulse and the fluence is investigated. We find that the transfer to the upper state can be dramatically enhanced over the zero chirp (high intensity) case for *both* directions of chirp: red to blue (positive chirp), in which the instantaneous frequency follows the energy ladder intervals, and, counterintuitively, also blue to red (negative chirp), for which the frequency does not follow the ladder.

The effect of chirping the optical pulses on the efficiency of population transfer can be visualized using the dressed-atom picture [12], shown in Fig. 1(b). The horizontal axis shows the excitation frequency, while the vertical axis displays the energies of the ladder states when ''dressed'' with a photon energy. The dashed lines in the figure portray the unperturbed dressed atom states $|1+\hbar\omega\rangle$, $|2\rangle$, and $|3-\hbar\omega\rangle$. When the dipole coupling between states $|1\rangle\leftrightarrow|2\rangle$ and $|2\rangle\leftrightarrow|3\rangle$ is included, as well as the second-order dipole coupling between states $|1\rangle\leftrightarrow|3\rangle$, the dressed-atom energies are modified as shown by the solid lines in the figure. In a chirped pulse, the instantaneous frequency changes during the pulse, which corresponds to a traversal of the dressed-atom diagram from left to right (red-to-blue chirp) or right to left (blue-to-red chirp). The precise manner by which the avoided transitions are traversed depends strongly on the excitation intensity and the rate of frequency sweep. At low intensity or rapid frequency changes, traversals tend to be *diabatic* and follow the dashed lines. However, at higher intensities and slower frequency sweep, the system can make an *adiabatic* traversal, for which the quantum state follows the solid curves.

For the three-state ladder system, there exist several paths by which to transfer population to the upper state $5d$. The most intuitive path is when the frequency is chirped from the red to the blue. Population transfer then occurs if the atom follows the fully adiabatic dressed atom curve, marked as path I in Fig. 1(b). It is important to note that essentially 100% population transfer occurs once the conditions for adiabatic passage have been met or exceeded (i.e., sufficiently high intensity and sufficiently low-frequency sweep rate). This is in marked contrast to population transfer via Rabi pumping, which is extremely sensitive to excitation intensity. For the intuitive chirp, another path is also important, denoted in the figure as path II. Here the system makes a diabatic traversal of the $|1\rangle\leftrightarrow|2\rangle$ transition, crosses to $|3\rangle$ adiabatically at the $|1\rangle\leftrightarrow|3\rangle$ two-photon transition, and then recrosses $|2\rangle$ diabatically. This path is important only at lower fluences, when path I does not lead to full transfer. In this case, paths I and II contribute to transfer to the upper state. The relative importance of the two routes depends on experimental parameters, but in general, a quantum-mechanical interference between the two routes will occur.

For counterintuitive blue-to-red chirped pulse, the situation is substantially different. Population cannot be transferred via sequential absorption of single photons. However, population can still be efficiently transferred via adiabatic crossing of the $|1\rangle\leftrightarrow|3\rangle$ two-photon transition, marked path III in the figure. Again, essentially full transfer to the upper state can be realized for all experimental parameters that meet or exceed the condition for adiabaticity for path III.

After the population is transferred to $|3\rangle$, another photon can be absorbed to leave the atom ionized. This process corresponds to a four-level ladder, with the top level in the continuum. The three-photon ionization signal is then used as a monitor of population transfer to the upper levels of the system. Two regions of parameter space have previously been studied experimentally in this ladder system. In one set of experiments, the low-intensity, perturbative limit was explored using amplified pulses from a Ti:sapphire laser [10]. The nature of the quantum-mechanical interference between paths I and II was investigated and it was shown that, for a

Gaussian spectrum, the interference lead to a sinusoidal beating of the upper-state population as a function of chirp. Full population transfer was not experimentally verified due to a lack of available laser fluence. In a separate series of experiments [11], the high-fluence regime was studied using square spectrum pulses. Full population transfer was measured for both directions of chirp. However, the spectrum was not broad enough to fully excite all transitions of the ladder. It was therefore necessary to change the center frequency of the laser when the laser chirp direction was changed.

In this paper we present measurements made on the rubidium quantum ladder as a function of excitation fluence and chirp. No other experimental parameters were varied during data collection. Consequently, it is possible to model the results using a single set of experimental parameters. We have been able to theoretically reproduce, in absolute magnitude and in functional form, the experimental results throughout the full range of conditions. In contrast to earlier studies [9,10], we were able to achieve complete population transfer for intuitive and counterintuitive chirp at the *same* settings of the laser and to investigate the transfer from the interfering pathway regime up to the adiabatic rapid passage regime. To present a clearer and more intuitive physical picture, we highlight the results from three important transition regimes.

(i) In the low-intensity limit, efficient transfer occurs only for intuitively chirped pulses. Furthermore, the modulation depth in the upper-state population as a function of chirp remains constant with increasing fluence. However, once the $|1\rangle \leftrightarrow |2\rangle$ crossing becomes fully adiabatic, path (I) will dominate at the expense of path II and will thus lead to the reduction and eventual disappearence of the population modulations. This transition is explored both theoretically and experimentally.

(ii) At intermediate fluences, population is efficiently transferred for both the intuitive and the counterintuitive chirp. For the intuitive red-to-blue chirp, the adiabaticity condition is independent of chirp; thus the population in the upper state approaches a constant level as chirp increases. However, theory predicts that the population transferred via the counter-intuitive chirp should tend toward zero with larger chirp values. This expectation is experimentally verified.

(iii) At very high fluences, essentially full population transfer is achieved with either direction of chirped pulses. In all cases, the efficiency of transfer is expected to be significantly higher than for the highest-intensity (zero-chirp) pulses. Experiments and theory confirm this picture.

This paper is organized as follows. In Sec. II we present the experimental technique and describe the apparatus used to perform the measurements. The experimental results are presented in Sec. III, along with an intuitive theoretical description of adiabatic passage. In Sec. IV we give a detailed comparison between theory and experiment, choosing data that highlight the three points enumerated above. We summarize our conclusions in Sec. V.

II. EXPERIMENTAL METHODS

The experimental setup is depicted schematically in Fig. 2. Rubidium atoms are evaporated in a vacuum system ($P \approx 10^{-7}$ Torr). In the interaction region the atomic beam is crossed with the linearly polarized laser beam. The laser source is based on a home-built Ti:sapphire oscillator. The self-mode-locked laser runs at ~780 nm with a bandwidth of ~9 nm. These infrared pulses are stretched and then used to seed a multipass Ti:sapphire amplifier [13]. After amplification, the pulses are recompressed. The position of maximum intensity (i.e., the position of zero chirp) is measured using a single-shot autocorrelator. The power spectrum of the laser is continuously monitored during the experiment with a grating spectrometer and a linear photodiode array.

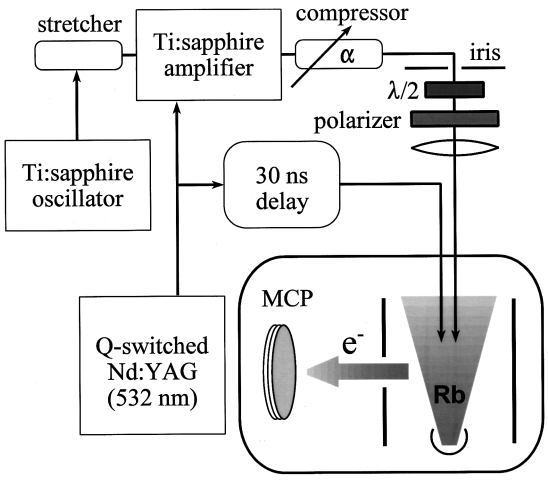

FIG. 2. Schematic of the experimental setup showing the laser system and interaction region. The chirp of the laser pulse was varied by adjustment of the compressor.

By adjusting the distance between the two gratings in the compressor, the linear chirp of the laser pulses can be continuously varied over a wide range of positive and negative chirp values. The amplified pulses are passed through an iris 3.7 mm in diameter (much smaller than the incident beam diameter) in order to provide an approximately flat intensity profile. A lens is used to image the iris onto the interaction plane with a magnification of $\frac{1}{2}$. Before the lens, the beam is passed through a rotatable half-wave plate and a linear polarizer in order to control the laser fluence in the interaction region. The relative fluence is monitored continuously with a fast photodiode; the absolute fluence is measured using a calibrated large area pyroelectric detector. The frequency-doubled output of a *Q*-switched Nd:YAG pulse (where YAG denotes yttrium aluminum garnet) is used to postionize any remaining population in the $5d$ state. The fluence of this pulse was carefully chosen such that it was of sufficient fluence to saturate the postionization signal, but lower than the fluence necessary to ionize the $5s$ or $5p$ state with a two-photon process. The photoionized electrons are pushed with a small electric field toward a multi-channel plate detector. The delay of the postionizing 532-nm pulse after the ir pulse is such that the two pulses of photoelectrons can be temporally resolved by the detector. All data presented in this paper, however, consist of a sum of these two signals, which is highly representative of the total population transferred to the $5d$ state. These data were collected using a computer-controlled digital oscilloscope. At each chirp point, typically 60 shots were recorded, of which only those shots with an ir fluence within 20% of the average were accepted. At each

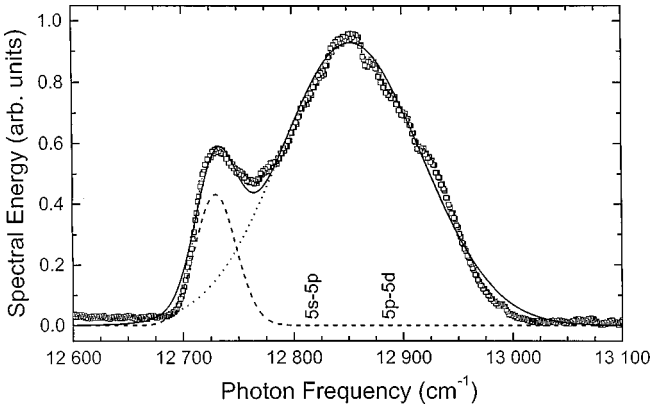

FIG. 3. Typical power spectrum for the excitation laser. The two solid lines represent a fit of the spectrum to two Gaussians. The main peak has a Gaussian width of 130 cm^{-1}, centered at 12 850 cm^{-1}. The side peak has about $\frac{1}{3}$ the width and about 15% of the area. Also shown are the two ladder transitions. Note that the side peak is far from either of the transitions. Only the central peak was used as input to the theoretical model.

fluence setting, a scan consisting of 20 chirp points was collected. Ionization data as a function of chirp was then collected at several values of fluence.

Analysis of the data requires understanding of the effect of the stretcher and compressor on the chirp of the optical pulse. It is a straightforward matter to calculate from the stretcher and compressor geometry the chirp placed on the pulse. We follow the derivation presented by Balling, Maas, and Noordam [10] and highlight the results. For a light pulse centered at ω_0 with a reasonably small bandwidth ($\Delta\omega \ll \omega$), the total phase shift can be expanded to second order in frequency or

$$\phi(\omega)=\phi_0+\frac{d\phi}{d\omega}(\omega-\omega_0)+\alpha(\omega-\omega_0)^2. \tag{1}$$

In this expression $d\phi/d\omega$ determines the group velocity of the pulse envelope and α describes the amount of chirp introduced by the pulse shaper. The time dependence of the outgoing pulse can be obtained simply

$$E_{\text{out}}(t)=\exp(-\Gamma t^2)\exp(i\omega_0 t), \tag{2}$$

where Γ is given by

$$\Gamma=\left[\frac{8\ln 2}{\Delta\omega^2}+4i\alpha\right]^{-1}. \tag{3}$$

We can see that for a Gaussian input pulse, the output pulse is also a Gaussian, with a carrier frequency that varies linearly in time, and a broadened pulse envelope, with a width given by

$$\tau^2=\tau_0^2+\left[\frac{8\ln 2\alpha}{\tau_0}\right]^2. \tag{4}$$

Thus, chirping has the effect of broadening the pulse. For large chirp values, the pulse is stretched approximately linearly with chirp:

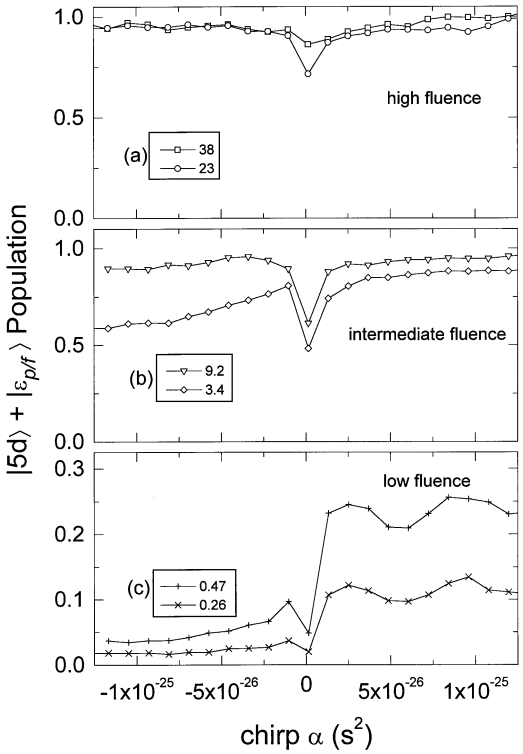

FIG. 4. Measured total photoelectron yield as a function of chirp at several different fluences: (a) 38 and 23 mJ/cm^2, (b) 9.2 and 3.4 mJ/cm^2, and (c) 0.47 and 0.26 mJ/cm^2. All of the data sets have been scaled vertically by a single parameter such that the largest signal corresponds to 100% population transfer to the upper state. Note the two horizontal scales: The lower corresponds to the chirp parameter, while the upper gives the broadening of the pulse, equal to $8\ln 2\alpha/\tau_0$. In (a) the full transfer can be seen for both signs of chirp, while only partial transfer exists at zero chirp. In (b) the fluence becomes too low to drive the two photon transition fully adiabatically, while in (c) the fluence has dropped to the point where modulation in the population is evident, due to quantum mechanical beating between paths I and II.

$$\tau\approx\frac{8\ln 2}{\tau_0}\alpha. \tag{5}$$

III. EXPERIMENTAL RESULTS

We begin by presenting spectral measurements made on the laser itself. A typical spectrum is shown in Fig. 3, along with the first two transitions of the anharmonic ladder. Ideally, the excitation laser would have a clean Gaussian spectrum. As can be seen from the figure, however, the spectrum exhibits a sharp feature on the red side of the line. This distortion is caused by bandwidth limitations in the stretcher and higher amplifier gain at longer wavelengths. The solid line in Fig. 3 represents a fit of two Gaussians to the measured spectrum. The sharp feature is well modeled by a narrow Gaussian with roughly 30% of the width and 15% of the energy of the main feature. Note that the center frequency of this side feature is well to the red of any ladder transition. We will further discuss the complications that this spectrum introduces to the analysis in Sec. IV.

Ionization data were collected as a function of chirp at six different fluences spanning over two decades, ranging from

0.25 to 38 mJ/cm^2. These data are summarized in Fig. 4. In Fig. 4(a), data taken at the highest fluences are displayed. Figure 4(b) displays data collected at intermediate fluences. Finally, Fig. 4(c) shows chirp scans taken at the highest available fluences. During the data collection only the chirp and the fluence were changed. In particular, the spectrum of the laser remained essentially constant. The relative scaling between the six scans was not adjustable; a single vertical multiplicative factor was used to normalize the data such that the largest ionization signal among all the data sets was scaled to unity.

The three transition regimes discussed in the Introduction are clearly apparent in the data. At the lowest fluences, the ionized population exhibits clear modulation as a function of chirp, caused by quantum interference between the two paths I and II. As the fluence is increased, we see that the modulation for positive chirp disappears. At the same time, we see the growing effectiveness of the counterintuitive chirp, until, at high fluences, a saturation of the transferred population is reached for both signs of the chirp. Perhaps most surprising is the fact that even at the highest fluences, the population transferred at zero chirp still has not reached saturation. Throughout the range of experimental parameters explored, chirping the pulse is *always* a more effective method of transferring population to the upper state of the anharmonic ladder. However, before a more detailed analysis of the data is presented, we first describe the theory used to model the results.

IV. ANALYSIS AND DISCUSSION

In order to understand the quantitative behavior of the interaction of the chirped pulses with the rubidium atoms, we will compare the data to a detailed theoretical model based on the numerical integration of the time-dependent Schrödinger equation. However, the discussion begins with a simpler analytic description of the process of adiabatic passage, so that a more clear physical intuition can be developed. Throughout this paper, we rely on a semiclassical approximation to the problem, in which the ladder system is treated fully quantum mechanically, but the optical pulse is described as a classical oscillating electric field.

For simplicity, we consider the problem of a two-level quantum oscillator. This general problem has been treated in great detail elsewhere [14]; in this forum, there is sufficient space to present only a few relevant results. The evolution of the system under the influence of the optical field is given by the precession of the Bloch vector (which describes the state of the quantum system) about a vector that characterizes the incident optical field. For direct on-resonance excitation, the two vectors are orthogonal, leading to large-amplitude precession of the state vector and thus 100% oscillations in the upper-state population. These oscillations are the so-called Rabi oscillations. However, if the excitation vector evolves sufficiently slowly and in the appropriate manner, it is possible to efficiently populate the upper state without the large oscillations characteristic of Rabi pumping. This process is called adiabatic passage. The criterion that must be satisfied for a passage to be fully adiabatic is given by the inequality

$$\frac{d\theta}{dt} \ll \sqrt{\Omega(t)^2+\Delta(t)^2}. \tag{6}$$

Here $\Omega(t)$ is the Rabi frequency, $\Delta(t)$ is the detuning of the carrier frequency from the transition frequency, and θ is the polar angle of the vector that describes the optical excitation. These are in turn given by the expressions

$$\Omega(t)=\frac{2d}{\hbar}\,\mathbf{E}(t), \quad \Delta(t)=\Delta(0)+\frac{d\omega}{dt}\,t, \qquad \theta(t)=\arctan\left(\frac{\Omega(t)}{\Delta(t)}\right), \tag{7}$$

in which $\mathbf{E}(t)$ is the electric-field envelope, d is the dipole oscillator strength of the transition, $\Delta(0)$ is the difference between the central frequency of the light pulse and the oscillator transition frequency, and $d\omega/dt$ describes the sweep of the carrier frequency in time within the pulse, i.e., the chirp. For a Gaussian spectrum and a linear chirp, $d\omega/dt$ is a constant.

It is illuminating to simplify Eq. (5) by assuming that the pulse envelope remains constant. Thus only the carrier frequency changes. Furthermore, examination of Eq. (5) clearly shows that the most critical period of time occurs in the vicinity of resonance, i.e., $\Delta \approx 0$. Making these two simplifications, Eq. (5) reduces to

$$\left|\frac{d\Delta}{dt}\right| \ll \Omega^2. \tag{8}$$

Thus a simple expression relating the frequency sweep rate to the incident electric field is obtained.

The prescription for adiabatic passage is simple. Begin with an optical field detuned far off resonance. The detuning Δ is large in this case and the angle between the state vector and the excitation vector is small. The state vector then precesses about the excitation vector. If the frequency sweeps slowly across the resonance (and the derivative of the intensity envelope is similarly small), then the rate of change of the angle θ can be slow enough compared to the precession frequency such that the inequality (5) is satisfied. If the carrier frequency continues to drift far past the resonance, then when the pulse ends the population is primarily in the upper state.

Although for a multilevel ladder the underlying physics remains unchanged, the picture becomes substantially more complex. It is therefore necessary to resort to numerical techniques to solve the problem. The theoretical model used to analyze these results is described in detail by Balling, Maas, and Noordam [10]. In this paper we present just an overview. The model is based on a five state system: $^2S_{1/2}$, $^2P_{3/2}$, $^2D_{3/2}$, $^2D_{5/2}$, and the continuum. Coupling between the levels is either obtained from reported oscillator strengths [15] or, in the case of coupling to the continuum, estimated based on modeling the atom as an electron in a Yukawa potential [16]. The coupled equations are solved by numerical integration over the duration of the frequency-chirped laser pulse. For a given chirp the population distribution over the five levels at the end of the ir laser pulse is determined. The sum of the population in the continuum and both $5d$ levels is computed for comparison to the experimental results.

These comparisons are presented in three different regions of parameter space, as described in the Introduction.

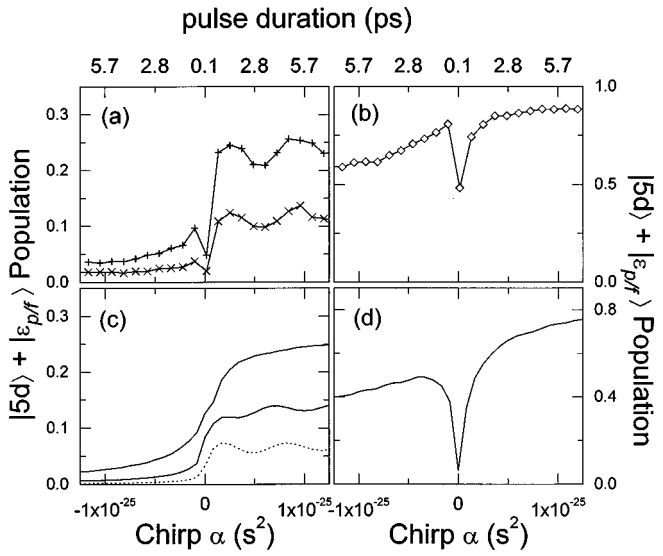

FIG. 5. Comparison between (a) and (b) data and (c) and (d) theory, showing the disappearance of the modulation beats with increasing fluence. Data are collected at three fluences: (a) 0.26 and 0.47 and (b) 3.4 mJ/cm^2. Below these are the results of theoretical modeling at four fluences: (c) 0.125, 0.25, and 0.5 and (d) 3.3 mJ/cm^2. Agreement is good between data and theory in both absolute magnitude and functional form.

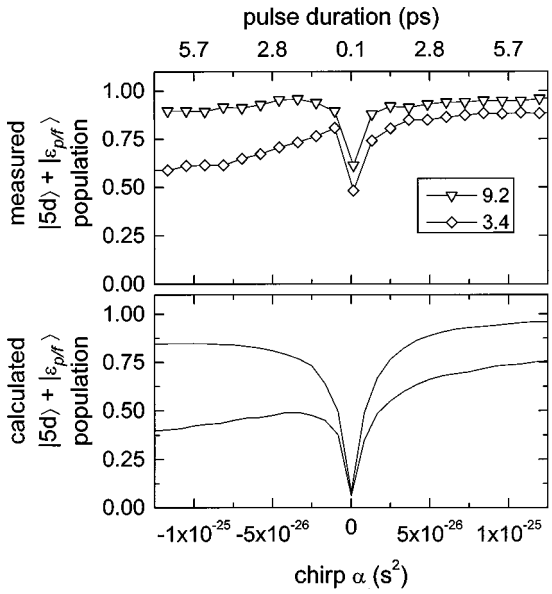

FIG. 6. Top panel: data collected at two fluences (3.4 and 9.2 mJ/cm^2), revealing the increasing efficiency of the counterintuitive blue-to-red chirp. Note the differences in asymptotic behavior between positive and negative chirps. Bottom panel: theory curves generated at two similar fluences (3.3 and 10 mJ/cm^2).

We begin with a study of the disappearance of the modulation beats that are evident at low fluence. The modulation eventually disappears when the 1-2 transition is crossed fully adiabatically. The fluence at which this occurs can be estimated from Eq. (7). We therefore examine data collected at roughly these fluences for evidence of the transition.

In Figs. 5(a) and 5(b) we display the total ionization signal as a function of chirp taken at three fluences: 0.26 and 0.47 mJ/cm^2 [Fig. 5(a)] and 3.4 mJ/cm^2 [Fig. 5(b)]. For the moment we concentrate on the signal at positive chirp values. The lowest two fluence scans, shown in Fig. 5(a), clearly display modulation in the population transfer, one of the hallmarks of the quantum interference between transfer paths I and II. For the highest fluence shown in Fig. 5(b), the modulations are no longer visible. Figures 5(c) and 5(d) show the results of theoretical modeling at four fluences: 0.125, 0.25, and 0.5 mJ/cm^2 [Fig. 5(c)] and 3.3 mJ/cm^2 [Fig. 5(d)]. Note that the functional form of the chirp scans is mimicked extremely well by the theoretical calculations. Theory and data also agree well in absolute magnitude.

There seems to be a slight disagreement between theory and data as to the precise fluence at which the modulations disappear, with the theory predicting a slightly lower value. The critical fluence is strongly dependent on the parameters of the excitation pulse. It is possible to bring theory and data into much closer agreement by slightly adjusting for each chirp scan the excitation pulse spectrum or fluence *within* measurement uncertainties. However, our goal in this paper is to explore and illuminate the competing processes of Rabi pumping and adiabatic passage. We have therefore used a single set of spectral parameters and one fluence calibration throughout in order to simplify the presentation of the results.

Next we study the transition region over which the counterintuitive chirp becomes important. Population transfer occurs via path III, shown in Fig. 1(b), which has a two-photon crossing that must be traversed adiabatically. The two-photon crossing behaves fundamentally differently from two sequential one-photon crossings. The difference is most easily seen in the asymptotic behavior of the transferred population at long chirps. We rewrite the simplified adiabaticity condition given by Eq. (7) as

$$R \equiv \frac{|(d\Delta/dt)|}{\Omega^2} \ll 1. \tag{9}$$

The asymptotic dependence of the ratio R on α is then studied. For large α, two things happen. First, the sweep rate decreases linearly with α. Second, the pulse gets longer [also linearly with α, as can be seen from Eq. (4)], implying that the electric-field amplitude decreases by a factor $\sqrt{\alpha}$. Thus, for single-photon transitions, the Rabi frequency Ω also decreases by $\sqrt{\alpha}$ [17]. Thus the ratio $R \rightarrow \alpha^{-1}/(\sqrt{\alpha})^{-2} \rightarrow 1$; that is, the adiabaticity condition for large intuitive chirp is independent of chirp. The situation for a two-photon crossing is different. In this case, the Rabi frequency depends on the *square* of the electric field [18]. Thus the adiabaticity ratio becomes $R \rightarrow \alpha^{-1}/(\alpha)^{-2} \rightarrow 1/\alpha$, which leads to a decrease in the population transfer efficiency with increasing counterintuitive chirp.

This effect can be clearly seen in Fig. 6. The top panel shows experimental data collected at two fluences: 3.4 and 9.2 mJ/cm^2. For positive chirps, the population saturates to a constant value with no sign of diminution. For negative chirps, however, the data collected at 3.4 mJ/cm^2 clearly decrease at more negative chirp values. Even the higher fluence scan tends to decrease as the chirp becomes more negative, although a longer chirp range would need to be covered for the effect to become more pronounced. The lower panel in the figure displays the predictions of the theory obtained at

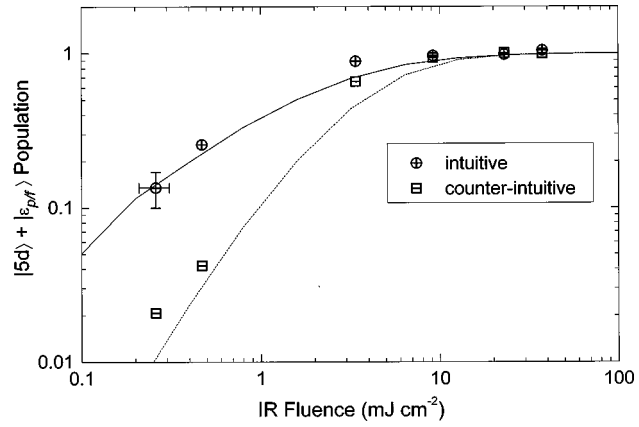

FIG. 7. Population transfer as a function of fluence for two specific chirp points: -7×10^{-26} s^2 (⊟) and 7×10^{-26} s^2 (⊕). The solid line shows the calculated populations at the positive chirp point, while the dashed line gives the theoretical result at the negative chirp point. Other than the single vertical scaling parameter used to set the measured saturation of population transfer to 100%, no other adjustable parameters have been used to fit the theory and the data.

roughly the same fluence values (3.3 and 10 mJ/cm^2). Again, the agreement is remarkable in both absolute magnitude and functional form. There appears to be some discrepancy between theory and experiment in the vicinity of zero chirp, the cause of which will be discussed later.

Finally, we discuss perhaps the most surprising result of all that, even at the highest fluence we were able to measure (38 mJ/cm^2), chirping the pulse is always a more effective means of population transfer than the high-intensity, zero-chirp pulse. It is possible to achieve essentially 100% population transfer even for counterintuitively chirped pulses, where the frequency sweep does not follow the ladder spacing. In Fig. 7 we display population transfer as a function of fluence for two specific chirp points: -7×10^{-26} and 7×10^{-26} s^2. The lines in the figure show the calculated populations at identical chirp values. The agreement is very good both in the low-fluence perturbative regime, where the population efficiency goes as the square of the fluence, and in the high-fluence region, where the transfer saturates at 100%. Only a single vertical scaling factor common to all data sets has been used such that the 100% transfer limit is reached at high fluence.

Only at zero chirp do the results deviate markedly from the measurements. Careful study of Figs. 5 and 6 reveal a similar trend: Agreement is best farther from zero chirp. The most likely explanation for these descrepancies lies in our model for the excitation pulse. We have modeled the optical pulse as a transform-limited Gaussian pulse. In reality, the pulse is a great deal more complicated, as can be seen from Fig. 3. The second subpeak on the red side of the main line contains about 15% of the total energy, which corresponds to substantial electric fields compared to the main peak. Therefore, the field interference between the two peaks can dramatically change the character of the incident near-infrared pulse and therefore change the efficiency of population transfer. Unfortunately, the power spectrum contains no phase information, so from the spectrum alone it is impossible to determine the precise incident field profile. However, chirping the pulse introduces a time ordering of the spectral components, such that the two features cease to interfere. Thus, at long chirps, the original phase information is irrelevant and the power spectrum is sufficient to describe the optical pulse. Exactly how much the pulse must be chirped before the effect of this side peak is negligible is difficult to determine without precise knowledge of the phase information of the incident spectrum. We estimate from the width of this subpeak that its corresponding field profile must be *at least* 600 fs, full width at half maximum, assuming that it is transform limited. This estimate is consistent with the observation that the model and data disagree within about 1 or 2 ps of zero chirp. Outside this region, where the power spectrum models the pulse sufficiently, agreement to the model is very good.

Furthermore, it is likely that at the highest intensities (small values of α) the theoretical model breaks down. As the optical field increases, the principle effect that occurs is that additional levels, such as the $^2P_{1/2}$ and the $7s$ state, are Stark shifted into resonance with the optical pulse. These levels not only affect the energy spacing of those levels included in the simplified ladder scheme, but also provide additional pathways for excitation and ionization. Thus it is perhaps not surprising that the present model underestimates the $5d$ population at zero chirp. However, given the uncertainty in the precise form of the excitation pulse, it is not possible to speculate further as to the cause of the deviations in the zero-chirp regime. A better understanding of these dynamics requires both a better-characterized infrared pulse and a more sophisticated theoretical model.

V. CONCLUSIONS

We have investigated population transfer as a function of pulse chirp in an anharmonic three ladder system from the perturbative regime up to fluences where 100% transfer occurs. It is seen that chirping the pulse such that the instantaneous frequency follows the ladder spacing is always a more effective means at population transfer to the upper state than is Rabi pumping at high intensity. Surprisingly, even a counterintuitive blue-to-red chirp also be more efficient than Rabi pumping. The results are analyzed in the context of adiabatic passage, which is found to be a robust and effective way to accomplish population transfer in ladder systems.

ACKNOWLEDGMENTS

We gratefully acknowledge the assistance of H. G. Muller for the operation and optimization of the amplified Ti:sapphire laser system. This work is part of the research program of the Stichting voor Fundamenteel Onderzoek der Materie (Foundation for Fundamental Research on Matter), and was made possible by financial support from the Nederlandse Organisatie voor Wetenschappelijk Onderzoek (Netherlands Organization for the Advancement of Research) and the Technology Foundation (STW).

[1] A. M. Weiner, J. P. Heritage, and E. M. Kirschner, J. Opt. Soc. Am. B **5**, 1563 (1988).
[2] W. S. Warren, H. Rabitz, and M. Dahleh, Science **259**, 1581 (1993).
[3] R. N. Zare, Nature (London) **365**, 105 (1993).
[4] For additional references see the feature issue, Proceedings of Femtosecond Chemistry, The Berlin Conference [J. Phys. Chem. **97**, 12 423 (1993)].
[5] S. Chelkowski, A. D. Bandrauk, and P. B. Corkum, Phys. Rev. Lett. **65**, 2355 (1990).
[6] A. Abragam, *The Principles of Nuclear Magnetism* (Oxford University Press, London, 1961), pp. 65–66.
[7] B. W. Shore, K. Bergmann, A. Kuhn, S. Schiemann, J. Oreg, and J. H. Eberly, Phys. Rev. A **45**, 5297 (1992).
[8] D. J. Maas, D. I. Duncan, R. B. Vrijen, W. J. van der Zande, and L. D. Noordam, Chem. Phys. Lett. **29D**, 75 (1998).
[9] R. B. Vrijen, D. I. Duncan, and L. D. Noordam, Phys. Rev. A **56**, 2205 (1997).
[10] P. Balling, D. J. Maas, and L. D. Noordam, Phys. Rev. A **50**, 4276 (1994).
[11] B. Broers, H. B. Van Linden van den Heuvell, and L. D. Noordam, Phys. Rev. Lett. **69**, 2062 (1992).
[12] R. Loudon, *The Quantum Theory of Light* (Clarendon, Oxford, 1983).
[13] R. Constatinescu, Ph.D. thesis, Free University, Amsterdam, 1997 (unpublished).
[14] L. Allen and J. H. Eberly, *Optical Resonance and Two-Level Atoms* (Dover, New York, 1987).
[15] A. A. Radzig and B. M. Smirnov, *Reference Data on Atoms, Molecules and Ions* (Springer-Verlag, Berlin, 1985).
[16] H. G. Muller, Ph.D. thesis, Free University, Amsterdam, 1985 (unpublished).
[17] L. Allen and J. H. Eberly, *Optical Resonance and Two-Level Atoms* (Ref. [14]), p. 54.
[18] L. Allen and C. Stroud, Phys. Rep. **91**, 1 (1982).